times because the transducer, in addition to producing a level difference, also produces a temperature difference between the two baths, ΔT, which is uniquely dependent on Z, the amount of fluid within the capacitor. We have shown that this reproducible variation of ΔT, or "structure," depends on Z rather than ΔZ (see Ref. 7). In addition, all of the various "peaks," local positive maxima of ΔT, have been studied as a function of frequency. The positions Z of these individual peaks all display an inverse relationship with the frequency of the ac sound field. The slopes observed, $-dZ/d\nu$, fall within the range (3 to 10) $\times 10^{-4}$ mm/Hz. Thus, the Z-ΔT "structure" produced by the transducer is not related to Josephson states.

[11]One could mistake some of these "steps" as the Josephson effect if the helium level were placed at the "right" value. For example, state E in Fig. 2 would appear to be the $n=1$ Josephson step if the initial $\Delta Z = 0$ level were raised by 0.38 mm.

[12]This dependence of the "steps" and ΔT "peaks" on frequency suggests that they may be explainable in terms of sound resonances within the annular region of the capacitor. This suggestion is further strengthened by the work of P. Leiderer [Diplomarbeit, Technischen Hochschule München, 1968 (unpublished)] and P. Leiderer and F. Pobell (private correspondence) who observed stable "steps" in the level difference for the geometry where the capacitor was replaced with a closed capillary. In that work the distance between successive "steps" was the wavelength of first sound rather than the expected Josephson relation. By comparison, the coaxial capacitor must be considered as a three-dimensional resonator, so that the spectrum for sound resonances is expected to be more complicated than for the capillary geometry. In particular, not only is there the possibility of standing waves in the dimension Z, but there is the added degree of freedom in the angular variable θ, i.e., standing waves about the annulus. The dimensions of the capacitor are such that one can fit up to thirteen wavelengths of first sound around the circumference of the annulus. In light of the added degrees of freedom for this three-dimensional resonator, the large number of ΔT "peaks" observed along with their range of values for $dZ/d\nu$ as well as the stable "steps" may be explainable in terms of sound resonances.

Effect of Magnetic Field on Electron Density Growth during Laser-Induced Gas Breakdown*

D. R. Cohn, W. Halverson, B. Lax,† and C. E. Chase
Francis Bitter National Magnet Laboratory,‡ Massachusetts Institute of Technology, Cambridge, Massachusetts 02139
(Received 4 October 1972)

The avalanche growth rate of CO_2-laser–induced gas breakdown in a magnetic field has been studied by measuring the time elapsed between the initiation of the laser pulse and the onset of observable breakdown effects such as a sharp decrease of laser transmission through the gas. The main features of the observed magnetic field dependence of this time difference can be explained in terms of the inhibition of electron diffusion from the laser focal region.

Considerable effort has been devoted to the study of the threshold pressure for laser-induced gas breakdown,[1] including recent investigations of the dependence of the threshold pressure upon magnetic field.[2] Very little attention, however, has been given to the study of the time evolution of the breakdown process.[3] In this paper we describe the first investigation of the influence of a magnetic field upon the time elapsed between the initiation of a laser pulse and the onset of observable breakdown effects such as the sharp decrease in laser transmission through the gas. The experimentally observed magnetic field dependence of this time of transmission decrease is compared with that predicted by a simple model of avalanche breakdown controlled by both free and ambipolar diffusion.

The experimental measurements were made by subjecting argon gas to focused 10.6-μm radiation from a 10-J CO_2 laser.[4] The laser was run without nitrogen in order to eliminate the long tail at the end of the pulse. The absence of the long tail made it possible to obtain more reproducible values of the transmission decrease time. With no nitrogen in the laser cavity, the laser pulses were reproducible to within 5–10%. The laser beam was directed through an NaCl beam splitter where about 15% of the radiation was directed to a reference germanium photon drag detector. The remainder of the beam passed through a CaF_2 attenuator and then through a lens of 10-cm focal length. The lens formed one end of a vacuum-tight stainless steel cylindrical cell 5 cm in diameter and 30 cm long which was positioned in the bore of a Bitter solenoid magnet. The direction of the magnetic field was parallel to the direction of the laser beam, which came to a focus in the center of the magnet. We estimate the radius of the beam at the focal spot to be about 300 μm. The laser power at the focal spot was about 10 MW. The transmission of the laser radiation was measured by a photon drag detector. A photomultiplier positioned behind a quartz window in the side of the breakdown chamber was used to detect visible radiation produced by the breakdown.

Curve *a* of Fig. 1 shows a typical oscilloscope trace of a laser pulse registered by the reference photon drag detector. Curve *b* shows the same pulse after it has been transmitted through 58 Torr of argon in a magnetic field of 7.3 kG. By comparing *b* to *a* one can see that a sharp decrease in the transmission of the laser radiation occurred about 80 nsec after the initiation of the laser pulse. The time of initiation of the laser pulse was determined to within ± 5 nsec by the intercept of the reference photon drag signal with the zero-signal abscissa on the oscilloscope.

In order to determine more accurately the time at which the decrease in transmission occurred, a differential amplifier was used to subtract the reference signal from the transmitted signal. With no gas in the cell, the magnitudes of the reference and transmitted photon drag signals were adjusted until the difference between them was close to zero. Thus any decrease in the transmitted signal due to the occurrence of breakdown was displayed as a positive signal. In Fig. 1, curve *c* shows the signal from the differential amplifier for the laser pulses shown in curves *a* and *b*. It can be seen that the point at which transmission decreases is then very clearly defined. The use of the differential amplifier was particularly valuable when the time of transmission decrease occurred near the end of the laser pulse. In this regime it was quite difficult to determine the point at which the transmission decreased from the transmitted pulse alone. The time of initiation of the laser pulse was determined by displaying both the reference laser pulse and the differential amplifier signal on a time-calibrated dual-beam oscilloscope.

The magnetic field dependence of transmission decrease time was measured in argon at several pressures close to the breakdown threshold pressure at zero magnetic field. The laser power

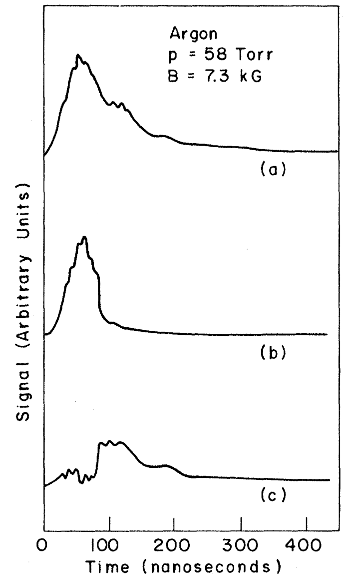

FIG. 1. Curve *a*, beam-split CO_2 laser pulse; curve *b*, transmitted laser pulse showing strong absorption at $t = 80$ nsec; curve *c*, transmitted signal subtracted from beam-split pulse by differential amplifier.

was held constant at 10 MW during all of the measurements. The zero-field breakdown threshold pressure was about 50 Torr. The experimentally observed magnetic field dependence of the time of transmission decrease at constant pressures of 48, 58, and 68 Torr is shown in Fig. 2. The spread of the times measured at a given value of magnetic field is indicated by the error bars. Measurements of the transmission decrease time at a pressure of 100 Torr showed that the magnetic field has a negligible effect at pressures far above the zero-field breakdown threshold pressure. The experimental measurements also indicated that the magnetic field only affected the time of transmission decrease when this time occurred near the end of the pulse at zero field.

The time elapsed before the observation of visible radiation was also studied. The magnetic field dependence of this time was found to be identical with that of the transmission decrease time. The visible radiation was not used for quantitative measurements because of the approximately 40-nsec electron transit delay of the photomultiplier tube.

The experimentally observed magnetic field dependence of the transmission decrease time can be understood in terms of an electron avalanche whose rate of growth is governed by the rate at which electrons diffuse out of the laser

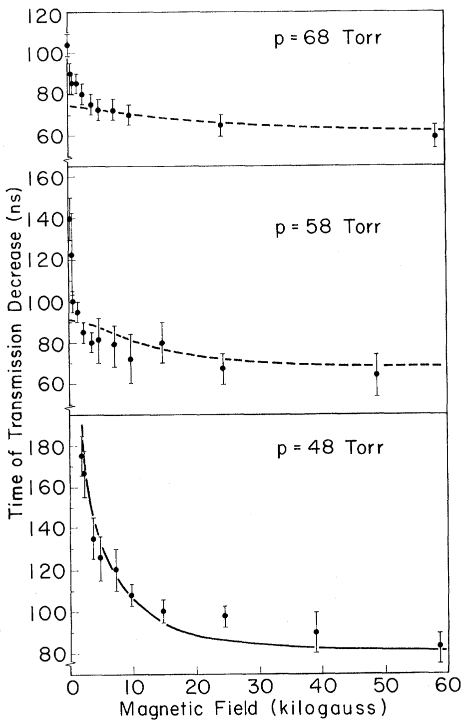

FIG. 2. Time of decrease of laser transmission as a function of magnetic field at argon pressures of 48, 58, and 68 Torr. Solid curve shows diffusion-controlled theory at $p=48$ Torr; dashed curves represent theory scaled for $p=58$ and 68 Torr.

focal spot. The change in laser-beam transmission occurs when the plasma density reaches some value n_f. The time t_f that must elapse before n_f is reached is given by

$$n_f = n_0 \exp\{\int_0^{t_f}[\nu_g(t) - \nu_l(t)]\,dt\}, \tag{1}$$

where n_0 is the initial electron density at time $t=0$, ν_g is the rate at which electrons are produced by the absorption of the laser radiation, and ν_l is the rate at which they are lost from the focal spot. We will assume that the loss occurs by free diffusion until a time t_c when a high enough density n_c is reached so that ambipolar diffusion is dominant. Since a magnetic field inhibits the free diffusion rate perpendicular to the field, the rate of loss by free diffusion, ν_{lf}, is a function of magnetic field B. For the range of pressure and magnetic fields used in our experiment, the rate of loss by ambipolar diffusion is much smaller than ν_{lf} and is essentially independent of magnetic field. For the simplified case of a square laser pulse, t_f is then given to a good approximation by

$$t_f(B) \approx \frac{\ln(n_f/n_0)}{\nu_g} + \frac{\nu_{lf}(B)\ln(n_c/n_0)}{\nu_g[\nu_g - \nu_{lf}(B)]}. \tag{2}$$

For our experiment, n_c is approximately equal to 10^{11} cm^{-3}. We estimate n_f to be on the order of 5×10^{17} cm^{-3}. This value of n_f is determined by equating the absorption length of the laser radiation with the length of the focal region. The absorption length is calculated for absorption due to electron-ion collisions at $T_e \approx 4$ eV. We note that the time to transmission decrease t_f goes as $\ln n_f$; hence t_f is not very sensitive to the value chosen for n_f.

From Eq. (2) it is evident that the magnetic field should have a significant effect upon t_f when the denominator in the second term in Eq. (2) is small. This occurs when ν_{lf} is nearly equal to ν_g at zero magnetic field. Since $\nu_{lf}(B)$ decreases with increasing magnetic field, t_f will also decrease with increasing field, as seen in Fig. 2. If, however, ν_g is much greater than ν_{lf} at zero field, then the magnetic field should have little effect. The experimentally observed absence of magnetic effects at 100 Torr is consistent with this prediction. Saturation of the magnetic field dependence of the breakdown time will occur as the difference between ν_g and $\nu_{lf}(B)$ becomes large, or when the field is high enough so that end losses greatly exceed radial losses, thereby making ν_{lf} independent of magnetic field.

In order to make a quantitative comparison of the experimental data with theory, we have computed the electron density buildup given by Eq. (1), using a linear rise and an exponential decay to model the shape of the laser pulse. In the simplest approximation ν_g can be written as[5]

$$\nu_g(t) = e^2 W(t)/\epsilon_0 \pi c m_e \omega^2 U_i r^2 \tau, \tag{3}$$

where $W(t)$ is the laser power delivered at the focal spot of radius r, ω is the laser frequency, U_i is the gas ionization potential, τ^{-1} is the electron-atom collision frequency, and other symbols have conventional meanings in mks units. To a good approximation $\tau^{-1} = \beta p$, where β is a constant and p is the initial gas pressure. The rate of electron loss is calculated by assuming that the region where electrons are created is cylindrical with radius r and length z. By analogy with the microwave breakdown case we can approximate the loss rate as[5]

$$\nu_l(t) = D_{sr}/L_r^2 + D_{sz}/L_z^2. \tag{4}$$

Here D_{sr} and D_{sz} represent radial and axial "transition" diffusion coefficients which change from those for free electron diffusion to ambipolar diffusion as the electron density builds up.

L_r and L_z represent effective diffusion lengths in the radial and axial directions, respectively. D_{sr} and D_{sz} are determined by generalizing the zero-field transition diffusion coefficients[6] to include the effect of the magnetic field. For the range of magnetic fields and pressures employed in our experiments, D_{sr} and D_{sz} are to a good approximation related to the zero-field free electron and ion diffusion rates D_{0e} and D_{0i} by

$$D_{sr} \approx 2D_{i0} \frac{D_{e0}/(1+\omega_c^2\tau^2)+(\sigma/\epsilon_0)L_r^2}{2D_{i0}+(\sigma/\epsilon_0)L_r^2} \tag{5}$$

and $D_{sz} \approx D_{sr}(\omega_c = 0)$, where ω_c is the electron-cyclotron frequency, and σ is the electrical conductivity at the center of the plasma.

The solid curve of Fig. 2 shows the theoretical prediction at $p = 48$ Torr, assuming an electron temperature of 3.5 eV, $\beta = 4.4\times10^9$ (Torr sec)$^{-1}$, and $n_0 = 1$ mm^{-3}. Following the microwave analogy, we took $L_r = r/2.4 = 145$ μm and $L_z = z/\pi = 370$ μm. The dashed curves represent the predicted dependence for the other pressures, using the same discharge parameters. As can be seen from Eq. (2), the time for strong laser absorption is very sensitive to the difference between ν_g and $\nu_{lf}(B)$. This difference is strongly dependent upon the values taken for T_e and β. The value of T_e used to fit the 48-Torr data is in reasonable agreement with electron temperatures calculated for laser-produced plasmas during the density buildup.[7] These calculations show that T_e can be taken to be essentially constant during the period of density growth. T_e changes very little because of the constant energy loss due to the ionization. The value of β used in our fit is consistent with that deduced from other laser breakdown experiments in argon.[8] Although a good fit can be found for only one pressure (without varying the discharge parameters), the theoretical curves agree with the observation that the magnetic field has less effect as the pressure is increased. They also agree with the observed reduction of the transmission decrease time at higher pressures. That the pressure dependence of the time of observable breakdown effects cannot be scaled using a simplified diffusion-limited model is consistent with studies of breakdown thresholds at zero magnetic field.[9]

The authors wish to thank Kambiz Alavi and Steven M. Wolfe for their assistance in the experimental measurements and data analysis.

---

*Work supported by U. S. Air Force Office of Scientific Research.

†Also Department of Physics, Massachusetts Institute of Technology, Cambridge, Mass. 02139.

‡Supported by the National Science Foundation.

[1] A rather complete review of laser-produced breakdown studies is given by C. DeMichelis, J. Quant. Electron., 5, 188 (1969).

[2] D. R. Cohn, C. E. Chase, W. Halverson, and B. Lax, Appl. Phys. Lett. 20, 255 (1972).

[3] A. V. Phelps, in *Physics of Quantum Electronics*, edited by P. L. Kelley, B. Lax, and P. E. Tannenwald (McGraw-Hill, New York, 1966), p. 538 ff.

[4] Built by Lumonics Research Limited, Ottawa, Canada.

[5] S. C. Brown, *Introduction to Electrical Discharges in Gases* (Wiley, New York, 1966), Chap. 10.

[6] W. P. Allis and D. J. Rose, Phys. Rev. 93, 84 (1954).

[7] P. de Montgolfier, J. Phys. D: Brit. J. Appl. Phys. 5, 438 (1972).

[8] F. Morgan, L. R. Evans, and C. G. Morgan, J. Phys. D: Brit. J. Appl. Phys. 4, 225 (1971).

[9] D. C. Smith, Appl. Phys. Lett. 19, 504 (1971).